Author accepted manuscript, 14th May 2019

Characterisation of $P2Y_2$ receptors in human vascular endothelial cells using AR-C118925XX, a competitive and selective $P2Y_2$ antagonist

Running title: AR-C118925XX, a competitive $P2Y_2$ antagonist

Markie O. Muoboghare[1], Robert Drummond[1] and Charles Kennedy[1]

[1]Strathclyde Institute of Pharmacy & Biomedical Sciences, University of Strathclyde, 161 Cathedral Street, Glasgow G4 0RE, United Kingdom

Correspondence: Dr. C. Kennedy, Strathclyde Institute of Pharmacy & Biomedical Sciences, University of Strathclyde, 161 Cathedral Street, Glasgow G4 0RE, United Kingdom
Tel +44 (0)141 548 2664 Fax +44 (0)141 552 2562 E-mail c.kennedy@strath.ac.uk

Word count: Intro=476, Results=752, Discussion=1,499, Total=2,727

Acknowledgements: The authors thank Matthew Lee and Dr. Calum Wilson for their help and advice in visualising $hP2Y_2$ receptor expression.

Abbreviations

1321N1-$hP2Y_1$ - 1321N1 cells stably expressing the human $P2Y_1$ receptor; 1321N1-$hP2Y_2$ - 1321N1 cells stably expressing the human $P2Y_2$ receptor; 1321N1-$hP2Y_4$ - 1321N1 cells stably expressing the human $P2Y_4$ receptor; 1321N1-$hP2Y_{11}$ - 1321N1 cells stably expressing the human $P2Y_{11}$ receptor; 1321N1-$rP2Y_6$ cells - 1321N1 cells stably expressing the rat $P2Y_6$ receptor; 95% cl - 95% confidence limits; ADP - adenosine 5'-diphosphate; ATP - adenosine 5'-triphosphate; AU - arbitrary units; CRC - concentration-response curves; DR - dose-ratio; (NAM) - negative allosteric modulator; UDP - uridine 5'-diphosphate; UTP - uridine 5'-triphosphate

BACKGROUND AND PURPOSE

There is a lack of potent, selective antagonists at most subtypes of P2Y receptor. The aims of this study were to characterise the pharmacological properties of the proposed $P2Y_2$ receptor antagonist, AR-C118925XX, and then to use it to determine the role of $P2Y_2$ receptors in the action of the $P2Y_2$ agonist, UTP, in human vascular endothelial cells.

EXPERIMENTAL APPROACH

Cell lines expressing native or recombinant P2Y receptors were superfused constantly and agonist-induced changes in intracellular Ca^{2+} levels monitored using the Ca^{2+}-sensitive fluorescent indicator, Cal-520. This set-up enabled full agonist concentration-response curves to be constructed on a single population of cells.

KEY RESULTS

UTP evoked a concentration-dependent rise in intracellular Ca^{2+} in 1321N1- $hP2Y_2$ cells (EC_{50} = 82 nM). AR-C118925XX (10 nM-1 μM) had no effect *per se* on intracellular Ca^{2+}, but shifted the UTP concentration-response curve progressively rightwards, with no change in maximum (pA_2=8.43). The inhibition was fully reversible on washout. AR-C118925XX (1 μM) had no effect at native or recombinant $hP2Y_1$, $hP2Y_4$, $rP2Y_6$ or $hP2Y_{11}$ receptors. Finally, in EAhy926 immortalised human vascular endothelial cells, AR-C118925XX (30 nM) shifted the UTP concentration-response curve rightwards, with no decrease in maximum (K_B =3.0 nM).

CONCLUSIONS AND IMPLICATIONS

AR-C118925XX is a potent, selective and reversible, competitive $P2Y_2$ receptor antagonist, which inhibited responses mediated by endogenous $P2Y_2$ receptors in human vascular endothelial cells. As the only $P2Y_2$-selective antagonist currently available, it will greatly enhance our ability to identify the functions of native $P2Y_2$ receptors and their contribution to disease and dysfunction.

Keywords: AR-C118925XX, $P2Y_2$ receptor, competitive antagonist, endothelial cells

Bullet point summary

What is already known

- P2Y receptors are expressed throughout the body, but their functions are largely unclear
- There is a lack of potent, selective antagonists at most subtypes of P2Y receptor

What this study adds

- AR-C118925XX is a potent, selective and reversible, competitive $P2Y_2$ receptor antagonist
- AR-C118925XX inhibited responses evoked by UTP in EAhy926 immortalised human vascular endothelial cells

Clinical significance

- AR-C118925XX is the only potent, selective and competitive $P2Y_2$ antagonist currently available
- AR-C118925XX will help identify the functions of native $P2Y_2$ receptors and their contribution to disease

Introduction

P2Y receptors are a family of eight GPCR that mediate the actions of the endogenous nucleotides, adenosine 5'-triphosphate (ATP), adenosine 5'-diphosphate (ADP), uridine 5'-triphosphate (UTP) and uridine 5'-diphosphate (UDP) (Abbracchio *et al.,* 2006; Kennedy *et al.,* 2013; Refehi & Müller, 2018). They are expressed in cells and tissues throughout the body, but their physiological functions are largely unclear. In part, this is because the endogenous agonists all act at multiple P2Y subtypes, but the major factor is the low potency and selectivity of many of the available antagonists. Currently, potent, selective antagonists have only been developed for $P2Y_1$ (eg. MRS2179, MRS2279, MRS2500) and $P2Y_{12}$ (e.g. ticagrelor, cangrelor, clopidogrel) receptors (see Abbracchio *et al.,* 2006; Kennedy *et al.,* 2013). These played a major role in identifying physiological roles, such as that of $P2Y_1$ receptors in peristalsis in the gut (see Kennedy, 2015) and of $P2Y_1$ and $P2Y_{12}$ receptors in platelet aggregation (Abbracchio *et al.,* 2006; von Kügelgen, 2017). Clearly, the development of potent and selective antagonists at the other P2Y subtypes would greatly enhance our ability to determine their functions in health and disease.

AR-C118925XX was developed by AstraZeneca around 20 years ago as a $P2Y_2$ antagonist, but only a conference abstract was published at the time (Meghani, 2002), which did not include crucial pharmacological properties, such as its K_B or pA_2. Several studies have since been published that used AR-C118925XX to investigate the role of native $P2Y_2$ receptors in the actions of P2Y agonists in various cell types (Kemp *et al.,* 2004; Hochhauser *et al.,* 2013; Onnheim *et al.,* 2014; Magni *et al.,* 2015; Wang *et al.,* 2015; Cosentino *et al*., 2016; Gabl *et al.,* 2016; see also review by Refehi & Müller, 2018). They did not, however, report the K_B or pA_2 of AR-C118925XX, or relate the concentrations used (mostly 1 and 10 µM) to its potency or selectivity. Inhibition of other P2Y subtypes could not, therefore, be ruled out based on the data published at this time.

Accurate values of antagonist potency are essential for effective experimental use. Recently, AR-C118925XX became commercially available, so the aims here were to quantify the pA_2 of AR-C118925XX at recombinant $P2Y_2$ receptors stably expressed in a cell line. Selectivity was then determined by studying its effects at other P2Y subtypes. Finally, AR-C118925XX was used to investigate native $P2Y_2$ receptors in human vascular endothelial cells. Using a system that enabled full agonist concentration-response curves (CRC) to be constructed in the absence and presence of AR-C118925XX on a single population of cells, we found that AR-C118925XX is a very potent, selective and reversible $P2Y_2$ receptor antagonist. Furthermore, it inhibited responses evoked by UTP in human vascular endothelial cells, indicating expression of endogenous $P2Y_2$ receptors. Thus the development of AR-C118925XX and characterisation of its pharmacological properties removes a substantial barrier to our ability to identify the functions of native $P2Y_2$ receptors.

Methods and Materials

Cell culture

1321N1 (ECACC Cat# 86030402, RRID:CVCL_0110) is a human astrocytoma cell line that does not endogenously express any of the eight P2Y receptor subtypes or respond to the naturally-occurring nucleotide agonists, such as UTP and ATP (Filtz *et al.,* 1994; Parr *et al.,* 1994; Abbracchio *et al.,* 2006). 1321N1 cells stably expressing recombinant human $P2Y_1$ (1321N1-$hP2Y_1$), $hP2Y_2$ (1321N1-$hP2Y_2$), $P2Y_4$ (1321N1-$hP2Y_4$), $P2Y_{11}$ (1321N1-$hP2Y_{11}$) or rat $P2Y_6$ (1321N1-$rP2Y_6$) receptors, tSA201 (ECACC Cat# 96121229, RRID:CVCL_2737) and EAhy926 cells (ATCC Cat# CRL-2922, RRID:CVCL_3901) were used. They were maintained in 5% CO_2, 95% O_2 in a humidified incubator at 37°C, in Dulbecco's Modified Eagles Media (Life Technologies, Paisley, UK, catalogue numbers 21969-035 - 1321N1, tSA201 cells, 41965-039 - EAhy926 cells), supplemented with 10% foetal calf serum, 1% non-essential amino acids, 1% penicillin (10,000 units/ml) and streptomycin (10 mg/ml). Prior to recording intracellular Ca^{2+}, the cells were plated onto 13 mm glass coverslips coated with poly-L-lysine (0.1 mg/ml) and experiments performed once a confluent monolayer of cells had developed. Experiments were performed unblinded and unrandomised, as the experimenter (MM) carried out all cell culture and was aware of which cell line was being used.

Ca^{2+} imaging

Cells were bathed in a buffer composed of (mM): NaCl 122; KCl 5; HEPES 10; KH_2PO_4 0.5; NaH_2PO_4 0.5; $MgCl_2$ 1; glucose 11; $CaCl_2$ 1.8, titrated to pH 7.3 with NaOH. Intracellular Ca^{2+} was monitored using the Ca^{2+}-sensitive fluorescent indicator, Cal-520. Cells on a coverslip were incubated for 1 hr at 37°C in the dark in buffer containing Cal-520-AM ester (5 μM) and Pluronic™ F-127 (0.05% w/v in DMSO). The coverslip was then placed vertically in the recording chamber of a Perkin Elmer LS50B luminescence spectrophotometer and the cells superfused continuously with buffer, applied under gravity at 4 ml min^{-1} and room temperature.

Cal-520 fluorescence, measured as arbitrary units (AU) in a population of cells, was sampled at 10 Hz following stimulation at 490±15 nm and the emission recorded at 525±15 nm using FL Winlab software (V4.00.02). Resting Ca^{2+} levels were stable over the course of the experiment. Agonists were added in the superfusate until the response reached a peak (60-90 sec) at 10 min intervals. For each drug addition, the data were exported to GraphPad Prism v7.01, GraphPad, San Diego, CA), where peak response amplitude was determined by the experimenter (MM) manually placing a cursor on the baseline and peak. All measurements were inspected and confirmed by CK.

Experimental protocols

The experimental protocols and design adhere to the recommendations of Curtis *et al.,* (2018).

Determining the effects of UTP and AR-C118925XX at hP2Y$_2$ receptors

This experimental set-up enabled full agonist CRC to be constructed on a single population of cells. All coverslips of 1321N1-hP2Y$_2$ cells were first exposed to UTP (1 μM) twice to confirm cell viability. CRC were then generated by superfusing cells with increasing concentrations of UTP at 10 min intervals, hence drug addition was not randomised. Reproducibility of these responses was determined by then generating a second CRC on the same population of cells. To facilitate comparison of the two curves, the data were normalised by calculating each response in AU as a percentage of that to UTP (1 μM) in the first CRC. This concentration is close to, but not quite at the top of the UTP CRC. The second CRC also served as a time-matched control for the effects of AR-C118925XX, as described next. EC_{50} and maximum values calculated by fitting the Hill equation to the two sets of data were compared using Student's paired t test.

The effects of AR-C118925XX at hP2Y$_2$ receptors were determined by generating two UTP CRC for each coverslip of 1321N1-hP2Y$_2$ cells. The first, to UTP alone, served as the control. The cells were then superfused with a given concentration of AR-C118925XX for 5 min. Thereafter, the second UTP CRC was constructed in the continuous presence of that concentration. Again, the data were normalised by calculating each response in AU as a percentage of that to UTP (1 μM) in the first CRC. The dose-ratio (DR) for the rightwards shift induced by AR-C118925XX was calculated from the EC_{50} values of the two curves. The data generated using a range of concentrations of AR-C118925XX were pooled and used to construct a Schild plot. To determine if the maximum responses to ADP was reduced by AR-C118925XX, the maximum values calculated by fitting the Hill equation to the second CRC were compared with those from the time-matched controls described in the previous paragraph, using one way ANOVA with Tukey's comparison.

Reversibility of the inhibitory effects of AR-C118925XX on washout were investigated by first exposing cells to UTP (1 μM) twice to confirm cell viability and then repeatedly adding UTP (100 nM), a concentration that is just above the EC_{50}, at 10 min intervals. Under these conditions, UTP (100 nM) elicits highly reproducible responses. Once a control response to UTP was obtained, AR-C118925XX was applied to the cells for 5 min, before co-administration with UTP. The antagonist was then washed out and the recovery of the UTP response monitored over the next 20-70 min, as appropriate. Since the point of this experiment was to determine if the responses fully recovered, the data were normalised by calculating the response in AU as a percentage of the control response to UTP. No statistical tests were applied to these data.

Selectivity of AR-C118925XX

In preliminary experiments, CRC for an appropriate agonist were constructed in cells expressing the other P2Y subtypes that couple to Ca^{2+} mobilisation and from these two concentrations were chosen that evoked responses that were i) close to the top of the CRC (reference concentration) and ii) 50-75% of the maximum response (test concentration), as follows: 1321N1-hP2Y_1 - ADP (1 μM/100 nM), 1321N1-hP2Y_4 - UTP (10 μM/1 μM), 1321N1-rP2Y_6 - UDP (1 μM/100 nM), 1321N1-hP2Y_{11} - ATP (10 μM /2 μM) and tSA201 cells - ADP (10 μM/1 μM). All coverslips were first exposed to the higher concentration of agonist twice to confirm cell viability. The response also served as a reference for statistical analysis, as described in the next paragraph. The lower, test concentration was then applied repeatedly at 10 min intervals and once a control response was obtained, AR-C118925XX (1 μM) was applied to the cells for 5 min before co-administration with the agonist.

Since the aim of this experiment was to determine if AR-C118925XX acts as an antagonist at the other P2Y subtypes, the data are presented as percentage of the agonist control response. To enable parametric statistical analysis, however, responses in a given cell line to the agonist test concentration were calculated as a percentage of the initial response to the agonist reference concentration. The values obtained in the absence and then presence of AR-C118925XX were then compared using Student's paired t test.

Investigating the presence of P2Y_2 receptors in EAhy926 cells

Ca^{2+} imaging UTP CRC were constructed in the absence and presence of AR-C118925XX and analysed statistically in the same manner as described above for 1321N1-hP2Y_2 cells, except that i) cells were first exposed to UTP (10 μM) twice to confirm cell viability and ii) data were normalised by calculating each response in AU as a percentage of that to UTP (10 μM) in the first CRC.

Immunostaining P2Y_2 receptor protein expression was studied using a modified version of the methods we used recently to demonstrate P2Y_2 expression in rat isolated carotid arteries (Lee *et al.,* 2018). Briefly, cells were fixed in 4% paraformaldehyde for 20 min at room temperature, washed three times in 100 μM glycine solution, then three times with a buffer composed of (mM): NaCl 137; KCl 2.7; NaH_2PO_4 1.5; Na_2HPO_4 15.2, pH 7.4. Cells were permeabilised with 0.2% Triton-X100 in 5 mM NH_4Cl solution for 10 min and washed three times with buffer. They were then incubated in antibody buffer solution containing 5% BSA for 1 hr at room temperature, followed by three washes with antibody wash solution containing 5% BSA. Next, they were incubated with a rabbit anti-P2Y_2 receptor antibody (sc-20124, 1:100, Santa Cruz, Dallas, TX, USA) in buffer containing 5% BSA and 2% donkey serum, overnight at 4°C. They were then washed three times with antibody wash solution containing 5% BSA, followed by incubation with Alexa Fluor 488 donkey anti-rabbit antibody (Invitrogen, Carlsbad, CA, USA) in antibody buffer solution for 1 hr at room temperature, followed by three washes with antibody wash solution without BSA and finally incubated in buffer before imaging. Negative controls were performed in the absence of 1º or 2º antibody. To visualise their nucleus, cells were incubated in buffer containing 0.5 mg ml^{-1} DAPI.

The Alexa Fluor 488 antibody was excited using 488 nm wide-field epifluorescence illumination provided by a LED (CoolLED pE-300^{ultra}, CoolLED Ltd, Andover, UK) and visualised using a back-illuminated electron-multiplying charge coupled device (EMCCD) camera (iXon Life 888; Andor, Belfast, UK; 13 µm pixel size) through a 40X (oil immersion; numerical aperture 1.3; Nikon S Fluor) objective lens. Fluorescence emission was recorded at 10 Hz. Fluorescence illumination was controlled, and images (16-bit depth) captured, using ImageJ (National Institutes of Health, Bethesda, MD, USA). DAPI was excited at 365 nm and fluorescence recorded and visualised in the same way. Images (8 bit depth) were then analysed and prepared for publication using ImageJ.

Data and statistical analysis

The data and statistical analysis comply with the recommendations on experimental design and analysis in pharmacology (Curtis *et al.,* 2015). Experiments were designed to have an equal n per group within each protocol based on previous studies on the individual cell lines (Kennedy *et al*., 2000; Morrow *et al*., 2014) and preliminary experiments (Kennedy *et al*., unpublished). Coverslips were excluded if the initial responses to the high concentration of agonist were too small for responses to lower concentrations to be measured accurately and with confidence. Values in the text and figures refer to mean ± SEM or geometric mean with 95% confidence limits (95% cl) for EC_{50} values. When appropriate, CRC were fitted to the data by logistic (Hill equation), nonlinear regression analysis (GraphPad Prism v7.01, San Diego, CA), and EC_{50} and maximum values calculated. The Gaddum-Schild equation was used to calculate the dissociation constant (K_B) of AR-C118925XX in EAhy926 cells. Statistical analysis was performed using Student's paired or unpaired t test, or one way ANOVA, as appropriate and as described in each experimental protocol above. Differences were considered significant when $P<0.05$.

Drugs, materials and solutions

ATP (Na_2 salt, cat. no. A7699), ADP (Na salt, cat. no. A2754), UTP ($Na_3(H_2O)_2$ salt, cat. no. 94370) and UDP (Na salt, cat. no. U4125) (Sigma-Aldrich Co, Gillingham, Dorset, UK) were dissolved in deionised water as 10 mM stock solution. AR-C118925XX (Tocris, Bristol, UK) was dissolved in DMSO as a 10 mM stock. All were frozen immediately and stored at -20°C, then diluted in buffer on the day of use. This was performed unblinded, as the experimenter was aware of which compound was being diluted. Cal-520-AM ester **(**Life Technologies, Paisley, UK**)** was dissolved in DMSO as a 1 mM stock solution, frozen immediately and stored at -20°C. On the day of use, it was diluted in buffer, as described above. Pluronic™ F-127 (Life Technologies, Paisley, UK) was supplied as a 20% w/v solution in DMSO and stored at room temperature. DAPI was obtained from Fisher Scientific UK (Loughborough, UK). Common chemicals were supplied by Sigma-Aldrich Co, Fisher Scientific UK (Loughborough, UK) and VWR International, (Lutterworth, UK) and were of the highest purity available. 0.1% DMSO has no effect on Ca^{2+} levels or nucleotide evoked responses in 1321N1 cells expressing recombinant P2Y receptors (Kennedy, *unpublished observations*).

Nomenclature of targets and ligands

Key protein targets and ligands in this article are hyperlinked to corresponding entries in http://www. guidetopharmacology.org, the common portal for data from the IUPHAR/BPS Guide to PHARMACOLOGY (Harding *et al.,* 2018), and are permanently archived in the Concise Guide to PHARMACOLOGY 2017/2018 (Alexander *et al.,* 2017).

Results

Determination of the pA_2 of AR-C118925XX

The first aim of this study was to calculate the pA_2 value of AR-C118925XX at human $P2Y_2$ receptors. Initial experiments determined the potency of the $P2Y_2$ agonist, UTP, in 1321N1- $hP2Y_2$ cells and the reproducibility of its action. UTP (10 nM - 3 μM) evoked a concentration-dependent rise in intracellular Ca^{2+} with an EC_{50} = 82 nM (95% cl = 52 - 112 nM) (Figure 1A,B). There was no significant change in the EC_{50} of a second CRC generated on the same population of cells (107 nM, 95% cl= 51 - 163 nM), but the maximum response according to the fit of the Hill equation was significantly decreased from 103 ± 1% to 97 ± 1% of the response to UTP (1 μM) in the first CRC (Figure 1B).

Preincubation with AR-C118925XX (10 nM - 1 μM) had no effect *per se* on intracellular Ca^{2+} levels, but produced a progressive rightwards shift in the UTP CRC (Figure 2A). The inhibition was surmountable and there were no differences in the maxima of the second CRCs obtained in the absence and presence of AR-C118925XX. A Schild plot of these data has an X-intercept = -8.30 and slope = 0.985±0.028 (Figure 2B), giving a pA_2 = 8.43 Thus AR-C118925XX appears to be a potent, competitive antagonist at $hP2Y_2$ receptors.

Reversibility of the actions of AR-C118925XX

To determine if the inhibitory effects of AR-C118925XX are reversible on washout, UTP (100 nM), which is just above its EC_{50}, was applied repeatedly at 10 min intervals and evoked highly reproducible responses in the absence of AR-C118925XX (Figure 3). Coapplication of AR-C118925XX (30 nM - 1 μM), abolished the effect of UTP, but this recovered to time-matched control values when UTP was reapplied after AR-C118925XX washout. Thus the inhibitory actions of AR-C118925XX reverse fully on washout.

Selectivity of AR-C118925XX

The selectivity of AR-C118925XX was then investigated by determining the effects of 1 μM, a concentration that is 270 times greater than its K_B at $P2Y_2$ receptors (3.7 nM), at the other P2Y subtypes that couple to Ca^{2+} mobilisation. This high concentration had no effect on basal intracellular Ca^{2+} levels in any of the cell lines used, nor did it affect the rise evoked by ADP (1 μM) in tSA201 cells, a modified HEK-293 cell line that expresses endogenous $P2Y_1$ receptors (Shakya-Shrestha *et al.,* 2010) (Figure 4A,B). Likewise, AR-C118925XX did not inhibit responses mediated via recombinant $hP2Y_1$, $hP2Y_4$, $rP2Y_6$ or $hP2Y_{11}$ receptors stably expressed in 1321N1 cells (Figure 4B). Thus AR-C118925XX displays a high degree of selectivity for $P2Y_2$ receptors.

The presence of functional $P2Y_2$ receptors in EAhy926 endothelial cells

The final aim of this study was to determine the role of native $P2Y_2$ receptors in the actions of UTP. EAhy926 cells are an immortalised human vascular endothelial cell line (Edgell *et al.,* 1983) that we previously showed to be responsive to UTP (Graham *et al.,* 1996; Paul *et al.,* 2000). UTP (100 nM - 30 μM) increased intracellular Ca^{2+} in EAhy926 endothelial cells in a concentration-dependent manner (EC_{50} = 670 nM, 95% cl = 535 - 837 nM) (Figure 5A,B). There was no significant change in the EC_{50} value when a second CRC was then constructed on the same population of cells (EC_{50} = 680 nM, 95% cl = 506 - 912 nM), but the maximum response was significantly decreased from 108 ± 3% to 96 ± 4% of the response to UTP (10 μM) in the first CRC (Figure 5B).

Preincubation with AR-C118925XX (30 nM), a concentration that is less than 10-fold higher than its K_B at $P2Y_2$ receptors and substantially lower than the concentration that we showed above to be inactive at other P2Y-subtypes

1.5 orders of magnitude lower than

a concentration that is 270 times greater than its K_B at $P2Y_2$ receptors (3.7 nM)

had no effect on the basal intracellular Ca^{2+} level, but shifted the UTP curve rightwards (EC_{50} = 7.6 μM, 95% cl. = 4.4 - 13.2 μM), with no decrease in maximum response (92 ± 8% of the response to UTP (10 μM) in the first CRC) relative to that of the time-matched control (96 ± 4%) (Figure 5C). Gaddum-Schild analysis gave a K_B = 3.0 nM.

Expression of $P2Y_2$ receptors in EAhy926 endothelial cells

To support these pharmacological data, $P2Y_2$ receptor expression in EAhy926 cells was visualised using an anti-$P2Y_2$ antibody that was previously used to identify an immunoreactive band of the predicted molecular weight of the $P2Y_2$ receptor in Western blots of EA926hy cell lysates (Raqeeb *et al*., 2011). Furthermore, we recently demonstrated the same antibody displayed immunoreactivity in 1321N1-h$P2Y_2$, but not wild-type 1321N1 cells (Lee *et al.,* 2018). Figure 6A shows $P2Y_2$ receptor-like immunoreactivity in EAhy926 cells. Negative controls show a lack of staining when either the 2º or 1º antibody was omitted (Figure 6B,C).

Discussion

A major impediment to determining the functions of the majority of P2Y receptor subtypes is the lack of useful antagonists. By measuring changes in Ca^{2+} levels in cell lines expressing recombinant or native P2Y receptors, we demonstrated that AR-C118925XX is a very potent, selective and apparently competitive antagonist at the $P2Y_2$ subtype. Furthermore, by recording from a single population of constantly superfused cells, we were able to show that the inhibitory effects of AR-C118925XX reversed fully on washout. Finally, combining our knowledge of the pharmacological profile of AR-C118925XX, with demonstration of $P2Y_2$-like immunoreactivity, revealed functional expression of endogenous $P2Y_2$ receptors in human vascular endothelial cells. Thus AR-C118925XX is a powerful new tool for determining the functions of $P2Y_2$ receptors in health and disease and identifying new therapeutic targets.

Mode of action of AR-C118925XX

In this study, UTP evoked a concentration-dependent rise in cytoplasmic Ca^{2+} levels in 1321N1-h$P2Y_2$ cells, with an EC_{50} of 82 nM, which is close the value (73 nM) we reported previously (Morrow *et al.,* 2014). AR-C118925XX did not affect basal Ca^{2+} levels on its own, but progressively shifted the UTP CRC rightwards, in a parallel manner and with no decrease in the maximum response. The slope of the Schild plot constructed from these data was almost one and the pA_2 was 8.43, equivalent to a K_B of 3.7 nM. Thus classical Schild analysis indicates that AR-C118925XX is a competitive $P2Y_2$ antagonist rather than a negative allosteric modulator (NAM). Thus far, however, the antagonist properties of AR-C118925XX have only been determined using Ca^{2+} changes as a bioassay. This is relevant because it is now clear that the apparent mode of antagonism of NAMs can vary depending upon the agonist used, the signalling pathway studied and the extent of signalling amplification. For example, BPTU, a $P2Y_1$ NAM, caused a progressive rightwards parallel shift of the 2-methylthioADP CRC, with no decrease in maximum, when inositol phosphate production or ERK1/2 stimulation were measured, but suppressed the maximum when β-arrestin2-mediated $P2Y_1$ receptor internalisation was studied (Gao and Jacobson, 2017). Furthermore, BPTU had a different activity profile against another $P2Y_1$ agonist. This biased functional antagonism suggests that each signalling event may be mediated via a specific receptor conformation.

In the present study, AR-C118925XX had no effect on resting Ca^{2+}. This is important because superfusion-induced shear stress may induce release of ATP and UTP from endothelial cells, which can then act in an autocrine/paracrine manner to stimulate P2Y receptors in the same or neighbouring cells (Wang *et al*., 2015; Burnstock, 2017). The lack of effect indicates that either superfusion did not induce nucleotide release or, if it did, the flow rate was fast enough to wash the nucleotides away from the cell surface and so prevent $P2Y_2$ receptor activation. This is consistent with other projects in our laboratory using constant superfusion. In no instance has an antagonist that inhibits an agonist-induced rise in Ca^{2+}, caused any change in resting Ca^{2+} level in cells expressing native or recombinant P2Y receptors (Kennedy, *unpublished observations*).

While this report was in preparation, Rafehi *et al.,* (2017a) published an improved procedure for synthesis of AR-C118925XX and details of its pharmacological actions at $hP2Y_2$ receptors expressed in 1321N1 cells. It is notable that the reported potency of AR-C118925XX (pA_2=7.43, K_B=37.2 nM) is an order of magnitude lower than ours. Furthermore, it appeared to increase the maximum response induced by UTP and the Schild slope (0.816) was substantially less than one. Interestingly, in a subsequent study, Rafehi *et al*., (2017b), the IC_{50} of AR-C118925XX against responses evoked by the EC_{80} of UTP was 62.9 nM. EC_{80} is theoretically 4 times EC_{50}, which was 5.61 nM. Applying the Cheng-Prusoff equation generates a K_B for AR-C118925XX of approximately 13 nM, which is closer to the value calculated here. Shortly afterwards, a group from AstraZeneca described the original design and synthesis of AR-C118925XX and reported pA_2 and K_B values of 7.8 and 15.8 nM respectively at $hP2Y_2$ receptors expressed in Jurkat cells (Kindon *et al.,* 2017). Neither the Schild plot nor the slope of the plot were included, however, so the mode of antagonism cannot be confirmed.

The biggest methodological difference between our study and those of Rafehi *et al.,* (2017a,b) and Kindon *et al.,* (2017) is that they used multi-well plates and a microplate reader to record changes in cytoplasmic Ca^{2+} levels. To generate a CRC, multiple populations of cells were stimulated once only, with a single concentration of UTP. In contrast, we constantly superfused a single population of cells, first generating a control CRC by repeatedly applying UTP in increasing concentrations and then repeating the process in the presence of AR-C118925XX. This is analogous to organ bath-type studies, where multiple sets of data can be generated on a single tissue. Such systems have an inbuilt control and less variability than microplate readers, which may be why our Schild plot slope was close to one. Disadvantages are that superfusion uses more drug and takes longer to generate data. Unsurprisingly, multi-well plates and microplate readers are much more widely used, but their limitations do need to be noted and considered. Accurate determination of antagonist K_B values is essential when considering an effective concentration of antagonist to use when studying native receptors in healthy and diseased cells and tissues.

Selectivity of AR-C118925XX

In this study, 1 μM AR-C118925XX, a concentration 270-times greater than its K_B, had no effect at

$P2Y_1$, $P2Y_4$, $P2Y_6$ or $P2Y_{11}$ receptors, so AR-C118925XX is highly selective for $P2Y_2$ receptors over the other P2Y subtypes that mobilise Ca^{2+}. This is important, as the endogenous P2Y agonists have complex pharmacological profiles and each stimulates at least two of the eight subtypes. UTP activates not only $P2Y_2$, but also $P2Y_4$ and possibly $P2Y_6$ receptors (Abbracchio *et al*., 2006; Guns *et al*., 2006; Bar *et al*., 2008; Kennedy *et al.,* 2013; Haanes *et al*., 2016; Refehi & Müller, 2018), so sensitivity of a cell or tissue to UTP isn't proof of $P2Y_2$ receptor expression. Furthermore, no $P2Y_4$ antagonists are currently commercially available, and whilst the $P2Y_6$ antagonist, MRS2578, has reasonably high potency, its action is non-surmountable and irreversible (Mamedova *et al.,* 2004) and effects at sites other than $P2Y_6$ receptors have been noted (Mitchell *et al.,* 2012). Kemp *et al*., (2004) reported that 10 μM AR-C118925XX had no effect at 37 other GPCR and ion channels. The only clear indication of an off-target action of sub-μM concentrations is at P2X3 receptors, with an IC_{50} of 819 nM (Rafehi *et al.,* 2017a). The K_B was not calculated, however. Nonetheless, AR-C118925XX is clearly highly selective for $P2Y_2$ receptors and its introduction into the P2Y pharmacopoeia is a major advance in the purinergic field.

Native $P2Y_2$ receptors in human endothelial cells

We showed here that AR-C118925XX also inhibited the rise in Ca^{2+} evoked by UTP in human EAhy926 vascular endothelial cells, in a surmountable manner. The K_B, 3.0 nM, is close to that seen at recombinant $hP2Y_2$ receptors and 333-fold lower than a concentration (1 μM) that is inactive at other P2Y-subtypes. Thus UTP appears to act via $P2Y_2$ receptors to mobilise Ca^{2+} in EAhy926 cells. This is consistent with our demonstration of $P2Y_2$-like immunoreactivity and the detection of $P2Y_2$ mRNA and protein in these cells (Raqeeb *et al*., 2011).

UTP has long been known to have multiple actions on endothelial cells, including inducing inositol phosphate metabolism, Ca^{2+} mobilisation, PGI_2 and NO release and vasodilation (Needham *et al*., 1987; O'Connor *et al*., 1991; Ralevic *et al*., 1991; Raqeeb *et al*., 2011; Lustig *et al*., 1992; Motte *et al*., 1993; Wilkinson *et al*., 1993), but its site of action was unclear. As noted above, UTP stimulates several P2Y subtypes, and mRNA and, to a lesser extent protein, for most P2Y subtypes are found in endothelial cells (Burnstock & Knight, 2004; Erlinge & Burnstock, 2008). Some insight has been provided by $P2Y_2$ receptor knockout (Guns *et al*., 2006; Bar *et al*., 2008; Haanes *et al*., 2016) and knockdown (Raqeeb *et al*., 2011), but although these are powerful techniques, they have limitations. Potent, selective, competitive antagonists, like AR-C118925XX, have the advantages of ease of use and applicability in humans and are a powerful, complimentary tool for studying receptor function. We recently used the dual approach of AR-C118925XX and immunoreactivity to show that $P2Y_2$ receptors are present in rat carotid artery endothelial cells and couple to Ca^{2+} mobilisation (Lee *et al.,* 2018). Thus $P2Y_2$ receptors may be a major site of action of UTP in vascular endothelial cells in general.

Conclusion

$P2Y_2$ receptors are expressed in many tissues and cell types in humans, but the lack of useful antagonists has hindered determination of their physiological and pathophysiological roles. Nonetheless, potential therapeutic targets have been proposed, including colorectal cancer (Gendron *et al*., 2017), atherosclerosis, nephrogenic diabetes insipidus and osteoporosis (see Rafehi *et al*., 2017a; Rafehi & Müller, 2018). As the only potent, selective and competitive $P2Y_2$ antagonist currently available, AR-C118925XX will be invaluable in identifying native $P2Y_2$ receptor function and their relevance as a target for the development of novel therapeutic agents.

References

Abbracchio MP, Burnstock G, Boeynaems JM, Barnard EA, Boyer JL, Kennedy C, Fumagalli M *et al.* (2006). International Union of Pharmacology. Update of the P2Y G protein-coupled nucleotide receptors: from molecular mechanisms and pathophysiology to therapy. Pharmacol Rev 58: 281-341.

Alexander SPH, Christopoulos A, Davenport AP, Kelly E, Marrion NV, Peters JA *et al*. (2017). The Concise Guide to PHARMACOLOGY 2017/18: G protein-coupled receptors. Br J Pharmacol 174: S17-S129.

Bar I, Guns PJ, Metallo J, Cammarata D, Wilkin F, Boeynaems JM, Bult H, Robaye B (2008). Knockout mice reveal a role for $P2Y_6$ receptor in macrophages, endothelial cells, and vascular smooth muscle cells. Mol Pharmacol 74: 777-784.

Burnstock G (2017). Purinergic signaling in the cardiovascular system. Circ Res 120: 207-228.

Burnstock G, Knight GE (2004). Cellular distribution and functions of P2 receptor subtypes in different systems. Int Rev Cytol 240: 31-304.

Cosentino S, Banfi C, Burbiel JC, Luo H, Tremoli E, Abbracchio MP (2012). Cardiomyocyte death induced by ischaemic/hypoxic stress is differentially affected by distinct purinergic P2 receptors. J Cell Mol Med 16: 1074-1084.

Curtis MJ, Alexander S, Cirino G, Docherty JR, George CH, Giembycz MA *et al.* (2018). Experimental design and analysis and their reporting II: updated and simplified guidance for authors and peer reviewers. Br J Pharmacol 175: 987-993.

Curtis MJ, Bond RA, Spina D, Ahluwalia A, Alexander SP, Giembycz MA *et al.* (2015). Experimental design and analysis and their reporting: new guidance for publication in BJP. Br J Pharmacol 172: 3461-3471.

Edgell CJ, McDonald CC, Graham JB (1983). Permanent cell line expressing human factor VIII-related antigen established by hybridization. Proc Natl Acad Sci USA 80: 3734-3737.

Erlinge D, Burnstock G (2008). P2 receptors in cardiovascular regulation and disease. Purinergic Signal 4: 1-20.

Filtz TM, Li Q, Boyer JL, Nicholas RA, Harden TK (1994). Expression of a cloned P2Y purinergic receptor that couples to phospholipase C. Mol Pharmacol 46: 8-14.

Gabl M, Holdfeldt A, Winther M, Oprea T, Bylund J, Dahlgren C, Forsman H (2016). A pepducin designed to modulate P2Y2R function interacts with FPR2 in human neutrophils and transfers ATP to an NADPH-oxidase-activating ligand through a receptor cross-talk mechanism. Biochim Biophys Acta 1863: 1228-1237.

Gao ZG, Jacobson KA (2017). Distinct signaling patterns of allosteric antagonism at the $P2Y_1$

receptor. Mol Pharmacol 92: 613-626.

Gendron F-P, Placet M, Arguin G (2017). $P2Y_2$ receptor functions in cancer: A perspective in the context of colorectal cancer. In: Atassi M. (eds) Protein Reviews. Advances in Experimental Medicine and Biology, 1051, Protein Reviews 19: 91-106, Springer, Singapore.

Graham A, McLees A, Kennedy C, Gould GW, Plevin R (1996). Stimulation by the nucleotides, ATP and UTP of mitogen-activated protein kinase in EAhy926 endothelial cells. Br J Pharmacol 117: 1341-1347.

Guns PJ, Van Assche T, Fransen P, Robaye B, Boeynaems JM, Bult H (2006). Endothelium-dependent relaxation evoked by ATP and UTP in the aorta of $P2Y_2$-deficient mice. Br J Pharmacol 147: 569-574.

Haanes KA, Spray S, Syberg S, Jørgensen NR, Robaye B, Boeynaems JM, Edvinsson L (2016). New insights on pyrimidine signalling within the arterial vasculature - Different roles for $P2Y_2$ and $P2Y_6$ receptors in large and small coronary arteries of the mouse. J Mol Cell Cardiol 93: 1-11.

Harding SD, Sharman JL, Faccenda E, Southan C, Pawson AJ, Ireland S *et al.* (2018). The IUPHAR/BPS Guide to PHARMACOLOGY in 2018: updates and expansion to encompass the new guide to IMMUNOPHARMACOLOGY. Nucl Acids Res 46: D1091–D1106.

Kemp PA, Sugar RA, Jackson AD (2004). Nucleotide-mediated mucin secretion from differentiated human bronchial epithelial cells. Am J Resp Cell Mol Biol 31: 446-455.

Kennedy C. (2015). ATP as a cotransmitter in the autonomic nervous system. Auton Neurosci Basic and Clinical 191: 2-15.

Kennedy C, Chootip K, Mitchell C, Syed, NH, Tengah A (2013). P2X and P2Y nucleotide receptors as targets in cardiovascular disease. Future Med. Chem 5: 431-439.

Kennedy C, Herold CL, Qi A, Harden TK, Nicholas RA (2000). ATP, an agonist at the rat $P2Y_4$ receptor, is an antagonist at the human $P2Y_4$ receptor. Mol. Pharmacol 57: 926-931.

Kindon N, Davis A, Dougall I, Dixon J, Johnson T, Walters I, Thom S, McKechnie K, Meghani P, Stocks MJ (2017). From UTP to AR-C118925, the discovery of a potent non nucleotide antagonist of the P2Y2 receptor. Bioorg Med Chem Lett 27: 4849-4853.

Lee MD, Wilson C, Saunter CD, Kennedy C, Girkin JM, McCarron JG (2018). Spatially-structured cell populations process multiple sensory signals in parallel in intact vascular endothelium. Sci Signal 11: eaar4411.

Lustig KD, Erb L, Landis DM, Hicks-Taylor CS, Zhang X, Sportiello MG, Weisman GA (1992). Mechanisms by which extracellular ATP and UTP stimulate the release of prostacyclin from bovine pulmonary artery endothelial cells. Biochim Biophys Acta 1134: 61-72.

Magni G, Merli D, Verderio C, Abbracchio MP, Ceruti S (2015). $P2Y_2$ receptor antagonists as anti-allodynic agents in acute and sub-chronic trigeminal sensitization: role of satellite glial cells. Glia 63: 1256-1269.

Mamedova LK, Joshi BV, Gao ZG, Von Kügelgen I, Jacobson KA (2004). Diisothiocyanate derivatives as potent, insurmountable antagonists of $P2Y_6$ nucleotide receptors. Biochem Pharmacol 67: 1763-1770.

Meghani P (2002). The design of $P2Y_2$ antagonists for the treatment of inflammatory diseases: Abstract of papers, 224th ACS National Meeting, Boston, MA. MEDI-012. 2.

Mitchell C, Syed NH, Tengah A, Gurney AM, Kennedy C (2012). Identification of contractile $P2Y_1$, $P2Y_6$ and $P2Y_{12}$ receptors in rat intrapulmonary artery using selective ligands. J Pharmacol Exp Therap 343: 755-762.

Morrow GB, Nicholas RA, Kennedy C (2014). UTP is not a biased agonist at human $P2Y_{11}$ receptors. Purinergic Signal 10: 581-585.

Motte S, Pirotton S, Boeynaems JM (1993). Heterogeneity of ATP receptors in aortic endothelial cells. Involvement of P2y and P2u receptors in inositol phosphate response. Circ Res 72: 504-510.

Needham L, Cusack NJ, Pearson JD, Gordon JL (1987). Characteristics of the P2 purinoceptor that mediates prostacyclin production by pig aortic endothelial cells. Eur J Pharmacol. 134: 199-209.

O'Connor SE, Dainty IA, Leff P (1991). Further subclassification of ATP receptors based on agonist studies. Trends Pharmacol Sci 12: 137-141.

Onnheim K, Christenson K, Gabl M, Burbiel J.C. Müller CE, Oprea, TI, Bylund J *et al*. (2014). A novel receptor cross-talk between the ATP receptor $P2Y_2$ and formyl peptide receptors reactivates desensitized neutrophils to produce superoxide. Exp Cell Res 323: 209-217.

Parr CE, Sullivan DM, Paradiso AM, Lazarowski ER, Burch LH, Olsen JC, Erb L *et al.* (1994). Cloning and expression of a human P2U nucleotide receptor, a target for cystic fibrosis pharmacotherapy. Proc Natl Acad Sci USA 91: 3275-3279.

Paul A, Torrie LJ, M^c^Laren GJ, Kennedy C, Gould GW, Plevin R (2000). P2Y receptor-mediated inhibition of tumour necrosis factor-α-stimulated stress-activated protein kinase activity in EAhy926 endothelial cells. J Biol Chem 275: 13243-13249.

Rafehi M, Burbiel JC, Attah IY, Abdelrahman A, Müller CE (2017a). Synthesis, characterization, and in vitro evaluation of the selective $P2Y_2$ receptor antagonist AR-C118925. Purinergic

Signal 13: 89-103.
Rafehi M, Müller CE (2018). Tools and drugs for uracil nucleotide-activated P2Y receptors. Pharmacol Ther 190: 24-80.
Rafehi M, Neumann A, Baqi Y, Malik EM, Wiese M, Namasivayam V, Müller CE (2017b). Molecular recognition of agonists and antagonists by the nucleotide-activated G protein-coupled $P2Y_2$ receptor. J Med Chem 60: 8425-8440.
Ralevic V, Burnstock G (1991). Effects of purines and pyrimidines on the rat mesenteric arterial bed. Circ Res 69: 1583-1590.
Raqeeb A, Sheng J, Ao N, Braun AP (2011). Purinergic $P2Y_2$ receptors mediate rapid Ca^{2+} mobilization, membrane hyperpolarization and nitric oxide production in human vascular endothelial cells. Cell Calcium 49: 240-248.
Shakya Shrestha S, Parmar M, Kennedy C, Bushell T (2010). Two-pore potassium ion channels are inhibited by both $G_{q/11}$- and G_i-coupled P2Y receptors. Mol Cell Neurosci 43: 363-369.
von Kügelgen I (2017). Structure, pharmacology and roles in physiology of the $P2Y_{12}$ receptor. In: Atassi M. (eds) Protein Reviews. Advances in Experimental Medicine and Biology, 1051, Protein Reviews 19: 123-138, Springer, Singapore.
Wang S, Iring A, Strilic B, Albarrán Juárez J, Kaur H, Troidl K et al. (2015). $P2Y_2$ and Gq/G_{11} control blood pressure by mediating endothelial mechanotransduction. J Clin Invest 125: 3077-3086.
Wilkinson GF, Purkiss JR, Boarder MR (1993). The regulation of aortic endothelial cells by purines and pyrimidines involves co-existing P2y-purinoceptors and nucleotide receptors linked to phospholipase C. Br J Pharmacol 108: 689-693.

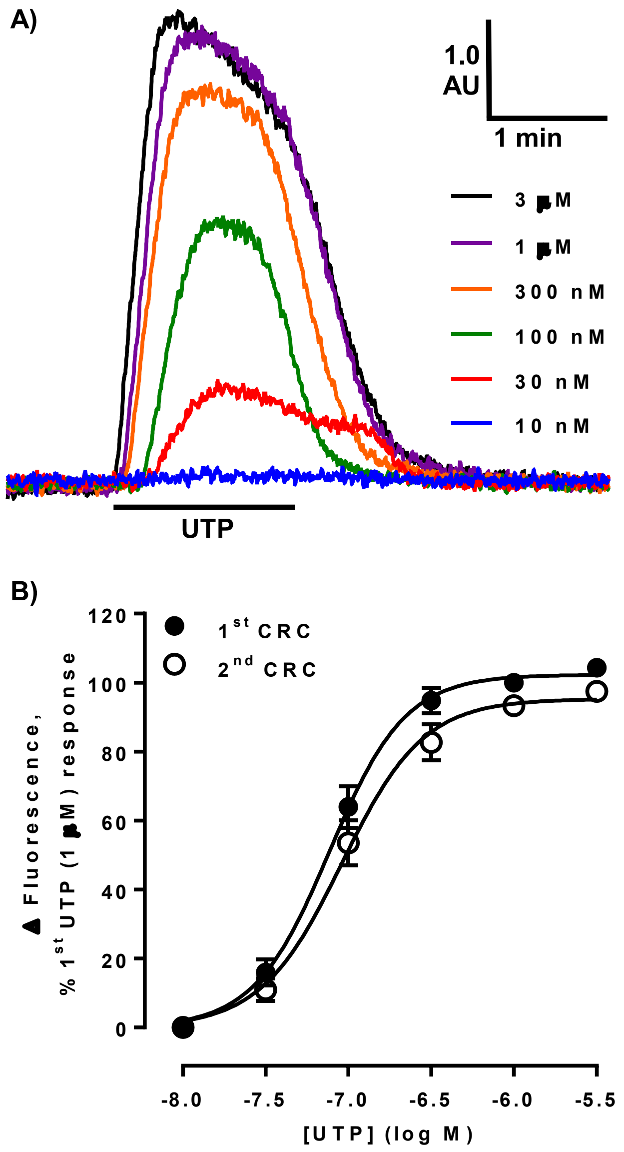

Figure 1 UTP elicits reproducible CRC in 1321N1-hP2Y$_2$ cells.

A) The superimposed traces show changes in Cal-520 fluorescence evoked by superfusion of cells with UTP (10 nM - 3 µM), as indicated by the horizontal bar. All records are from the same population of cells. B) The mean peak amplitude of responses evoked by UTP are shown (n=6). Two consecutive CRC were constructed per coverslip of cells. The data are expressed as a percentage of the response to UTP (1 µM) in the first CRC. Vertical lines show SEM. For some points, the error bars are shorter than the height of the symbol. The curves represent the fit of the Hill equation to the data.

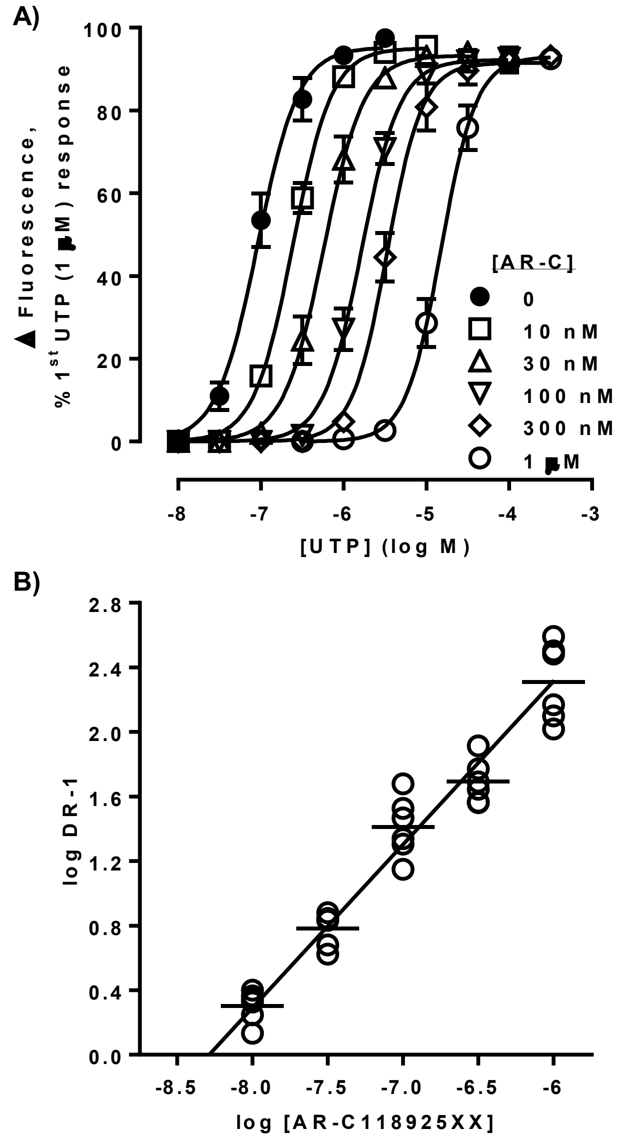

Figure 2 AR-C118925XX is a competitive antagonist at hP2Y$_2$ receptors.

A) The mean peak amplitude of responses evoked by UTP (10 nM - 300 µM) in 1321N1-hP2Y$_2$ cells in the absence and presence of AR-C118925XX (10 nM - 1 µM) is shown (n=6 each). The data are expressed as a percentage of the response to UTP (1 µM) in the control CRC for each coverslip of cells. Vertical lines show SEM. For some points, the error bars are shorter than the height of the symbol. The curves represent the fit of the Hill equation to the data. B) A Schild plot constructed from the data in panel A) is shown. The straight line represents the fit of the data by linear regression (r^2 = 0.0996). The horizontal lines indicate the mean of the values.

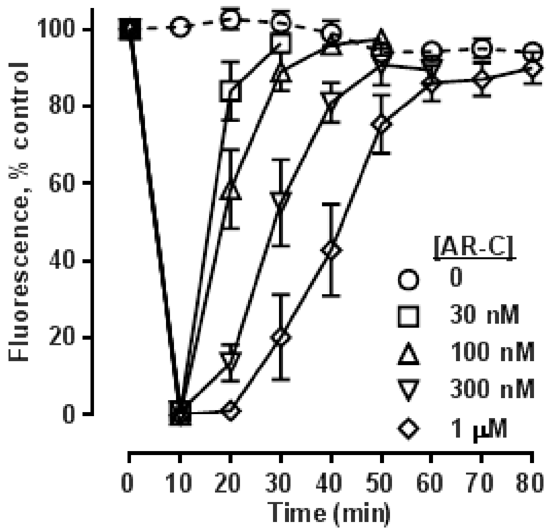

Figure 3 The inhibitory actions of AR-C118925XX are reversible.

The graph shows the time-course of responses evoked by repeated addition of UTP (100 nM) to 1321N1-hP2Y$_2$ cells at 10 min intervals in the absence (0 min), presence (10 min) and following washout of AR-C118925XX (30 nM - 1 µM) (20-80 min) (n=5 each). AR-C118925XX was added for 5 min as indicated by the horizontal bar. The data are expressed as a percentage of the control response to UTP, obtained before AR-C118925XX addition (0 min). The open circles and dashed line show the time-matched control when AR-C118925XX was not applied to the cells. Vertical lines show SEM.

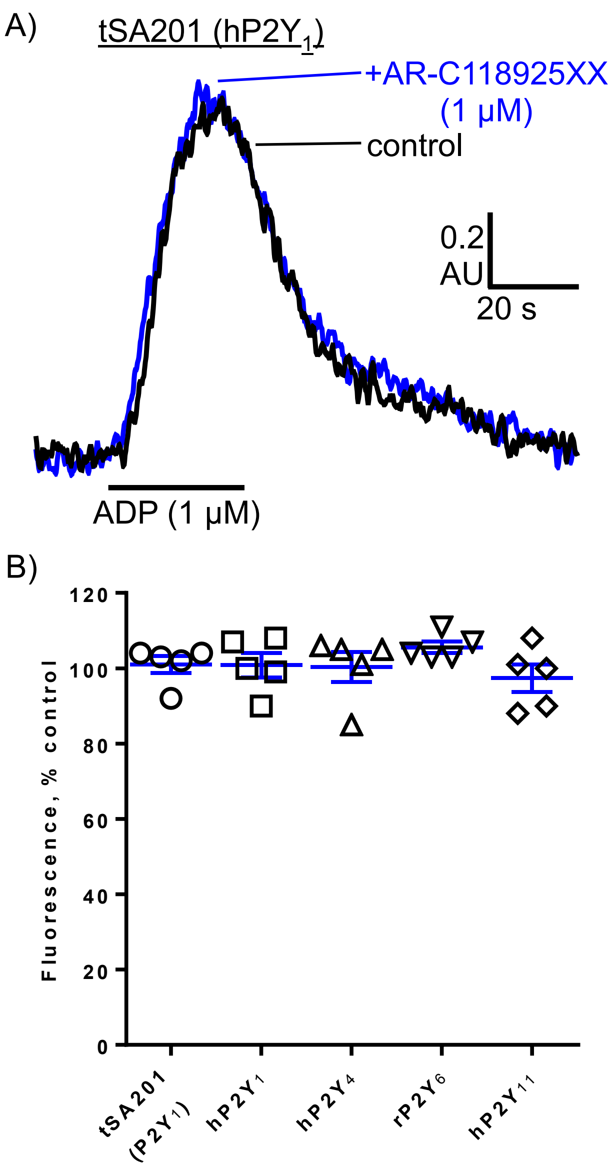

Figure 4 AR-C118925XX is selective for $hP2Y_2$ receptors.

A) The superimposed traces show changes in Cal-520 fluorescence evoked by superfusion of tSA201 cells with ADP (1 µM), as indicated by the horizontal bar, in the absence (black line) and presence (blue line) of AR-C118925XX (1 µM). All records are from the same population of cells. B) The peak amplitude of responses evoked by ADP (1 µM) in tSA201 cells, ADP (100 nM) in 1321N1-$hP2Y_1$ cells, UTP (1 µM) in 1321N1-$hP2Y_4$ cells, UDP (100 nM) in 1321N1-$rP2Y_6$ cells and ATP (2 µM) in 1321N1-$hP2Y_{11}$ cells in the presence of AR-C118925XX (1 µM) are shown (n=5 each). They are expressed as a percentage of the agonist control response, obtained before AR-C118925XX addition. The horizontal and vertical lines indicate mean and SEM.

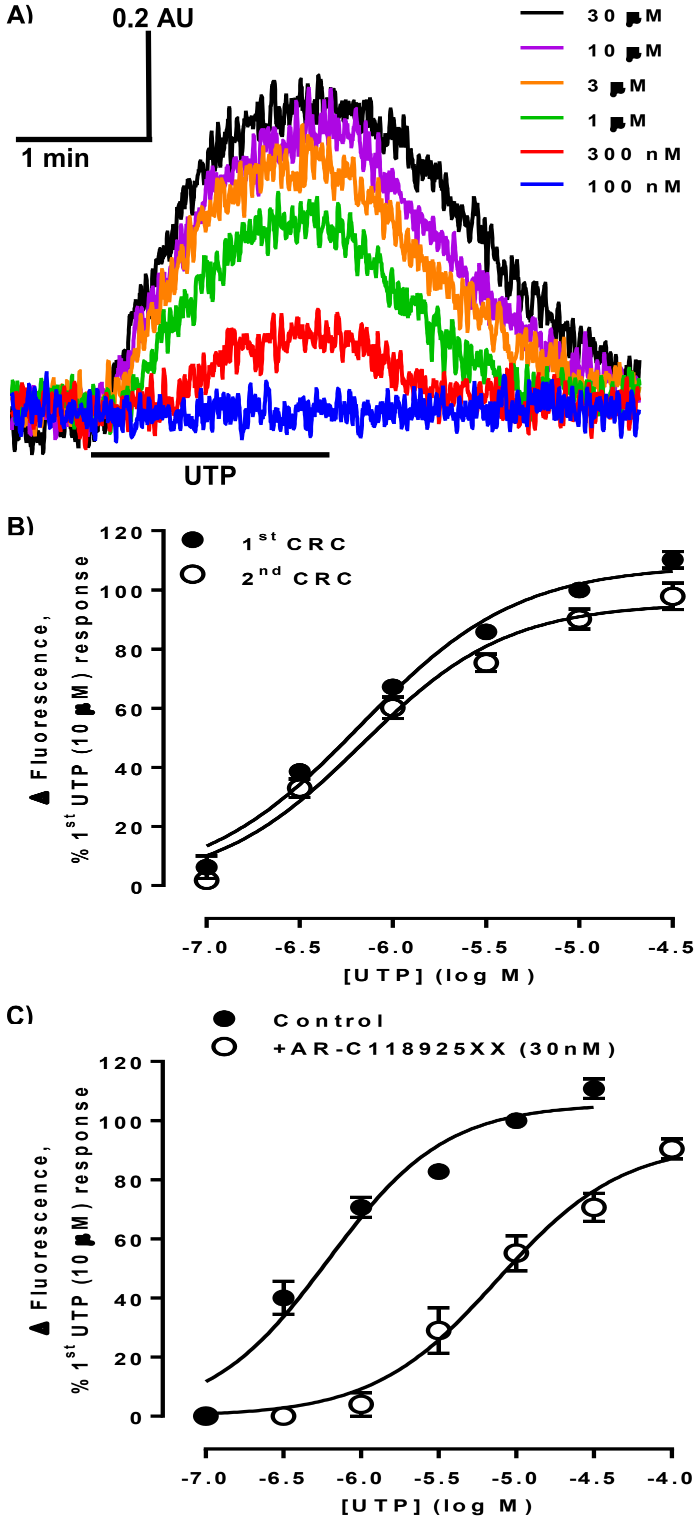

Figure 5 UTP acts at $P2Y_2$ receptors in EAhy926 endothelial cells.

A) The superimposed traces show changes in Cal-520 fluorescence evoked by superfusion of EAhy926 cells with UTP (100 nM - 30 µM), as indicated by the horizontal bar. All records are from the same population of cells. B) The mean peak amplitude of responses evoked by UTP (100 nM - 30 µM) when two consecutive CRC were constructed per coverslip of cells, is shown (n=5). C) shows the same when the 2nd curve was generated in the presence of AR-C118925XX (30 nM) (n=5). The data are expressed as a percentage of the response to UTP (10 µM) in the first CRC. Vertical lines show SEM. For some points, the error bars are shorter than the height of the symbol. The curves represent the fit of the Hill equation to the data.

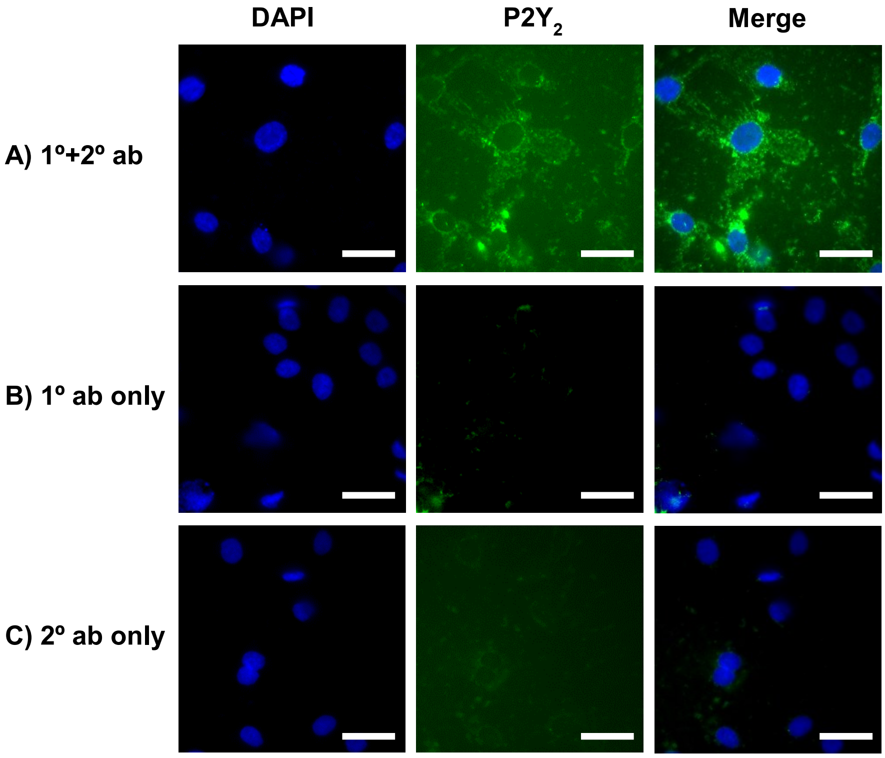

Figure 6 $P2Y_2$ receptor immunostaining in EAhy926 endothelial cells.
Representative images show; nuclear staining by DAPI (blue, left hand column), $P2Y_2$ receptor-like immunoreactivity (green, middle column) and overlay of both (right hand column), when cells were incubated with A) both 1° and 2° antibodies, B) the 1° antibody only and C) the 2° antibody only. Scale bars = 50 μm.